Twist-Angle-Dependent Ultrafast Charge Transfer in MoS_2-Graphene van der Waals Heterostructures

Duan Luo, Jian Tang, Xiaozhe Shen,* Fuhao Ji, Jie Yang, Stephen Weathersby, Michael E. Kozina, Zhijiang Chen, Jun Xiao, Yusen Ye, Ting Cao, Guangyu Zhang,* Xijie Wang,* and Aaron M. Lindenberg*

ABSTRACT: Vertically stacked transition metal dichalcogenide-graphene heterostructures provide a platform for novel optoelectronic applications with high photoresponse speeds. Photoinduced nonequilibrium carrier and lattice dynamics in such heterostructures underlie these applications but have not been understood. In particular, the dependence of these photoresponses on the twist angle, a key tuning parameter, remains elusive. Here, using ultrafast electron diffraction, we report the simultaneous visualization of charge transfer and electron−phonon coupling in MoS_2-graphene heterostructures with different stacking configurations. We find that the charge transfer timescale from MoS_2 to graphene varies strongly with twist angle, becoming faster for smaller twist angles, and show that the relaxation timescale is significantly shorter in a heterostructure as compared to a monolayer. These findings illustrate that twist angle constitutes an additional tuning knob for interlayer charge transfer in heterobilayers and deepen our understanding of fundamental photophysical processes in heterostructures, of importance for future applications in optoelectronics and light harvesting.

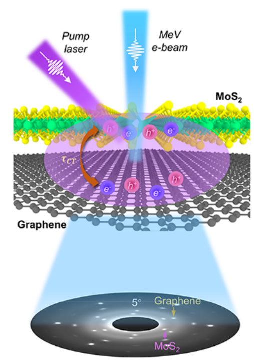

KEYWORDS: *van der Waals heterostructures, charge transfer, electron−phonon coupling, structural dynamics, ultrafast electron diffraction*

Van der Waals (vdW) heterostructures (HSs),[1] formed by vertically stacking different two-dimensional (2D) materials without lattice-matching constraints, offer a new paradigm for exploring new phenomena not observable in their component materials[2] and for tailoring device applications with novel functionalities.[3,4] A representative example is the atomically thin transition metal dichalcogenide (TMD)-graphene (Gr) vdW heterostructure, which combines the superior light−matter interaction of TMDs with the high carrier mobility of graphene, showing potential for next-generation optoelectronic devices, such as photodetectors,[5−10] photovoltaic devices,[11−15] and 2D electronics.[16−18]

Interlayer interactions between the adjacent layers, including ultrafast photoinduced interfacial charge transfer (CT)[19−21] and interlayer coupling involving phonons,[22−25] play a critical role in determining the emergent properties of these bilayer systems and their device performances. However, the underlying microscopic processes in this out-of-equilibrium regime are still mysterious. Remarkably, how the microscopic interactions evolve with the twist angle between neighboring layers remains largely unclear.

Recently, time-resolved optical spectroscopy techniques[13,14,22,26−31] have been extensively employed to investigate the ultrafast carrier transfer dynamics in TMD-Gr HSs. With different excitation conditions, graphene can act as both the injector and the collector of hot carriers with high quantum efficiency.[15] The interfacial electron transfer time has been measured to range from a few hundreds of femtoseconds to 1−2 ps[13,22,26−28] with above-bandgap excitation. An ultrafast hot carrier injection from graphene to TMDs has also been reported with sub-bandgap excitation.[13,14] Moreover, a slow (>100 ps) acoustic phonon recycling process[30] was found in WS_2-Gr HSs, which coupled photogenerated heat in graphene back into the carrier distribution in WS_2. Furthermore, when excited at resonance to the A-exciton in WS_2, a charge-separated transient state with a lifetime of ∼1 ps was found in an epitaxial WS_2-Gr HS by using time- and angle-resolved photoemission spectroscopy (tr-ARPES).[32] In sharp contrast to the ∼1 ps lifetime, very recent research reported a long-lived charge separation beyond 1 ns following ultrafast CT.[31] Despite numerous ultrafast studies on the electronic dynamics of TMD-Gr HSs, the dynamics of interfacial CT and its twist angle dependence remain elusive, and only indirect lattice dynamical information can be inferred from the aforementioned measurements. In addition to the interlayer CT, interlayer energy transfer in TMD-Gr HSs has been probed by photoluminescence (PL) and phonon-sensitive Raman

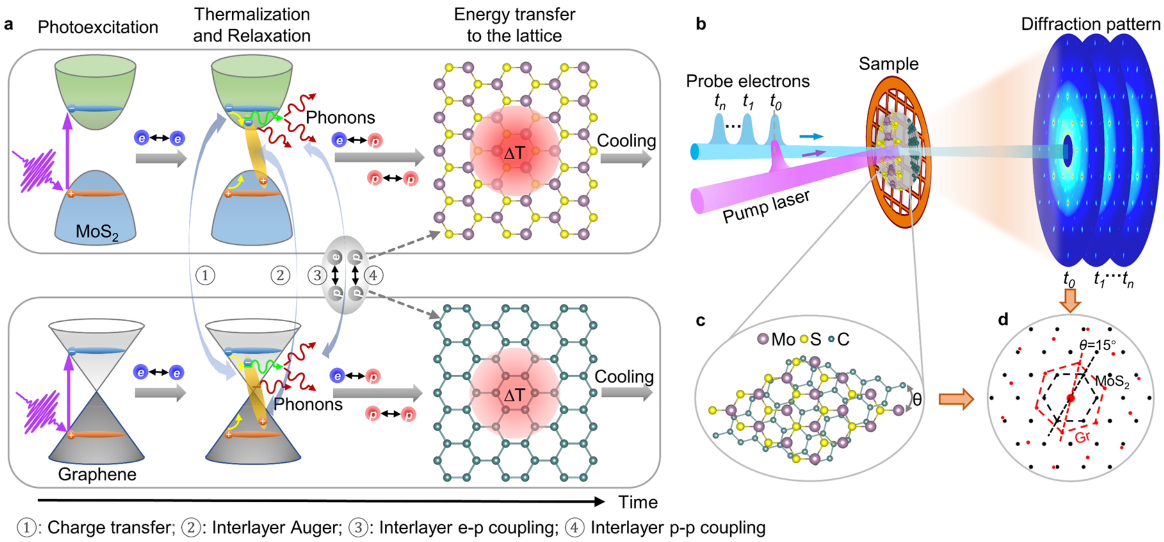

Figure 1. Fundamental photophysical processes in TMD-graphene heterostructures. (a) Illustration of the coupling between the two different electronic and lattices systems. (b) Schematic representation of experimental method. (c) Top view of the heterostructure with a twist angle of θ. Mo, S, and C atoms are presented as purple, yellow, and green spheres, respectively. (d) Simulated diffraction pattern of the 15° MoS_2-graphene heterostructure.

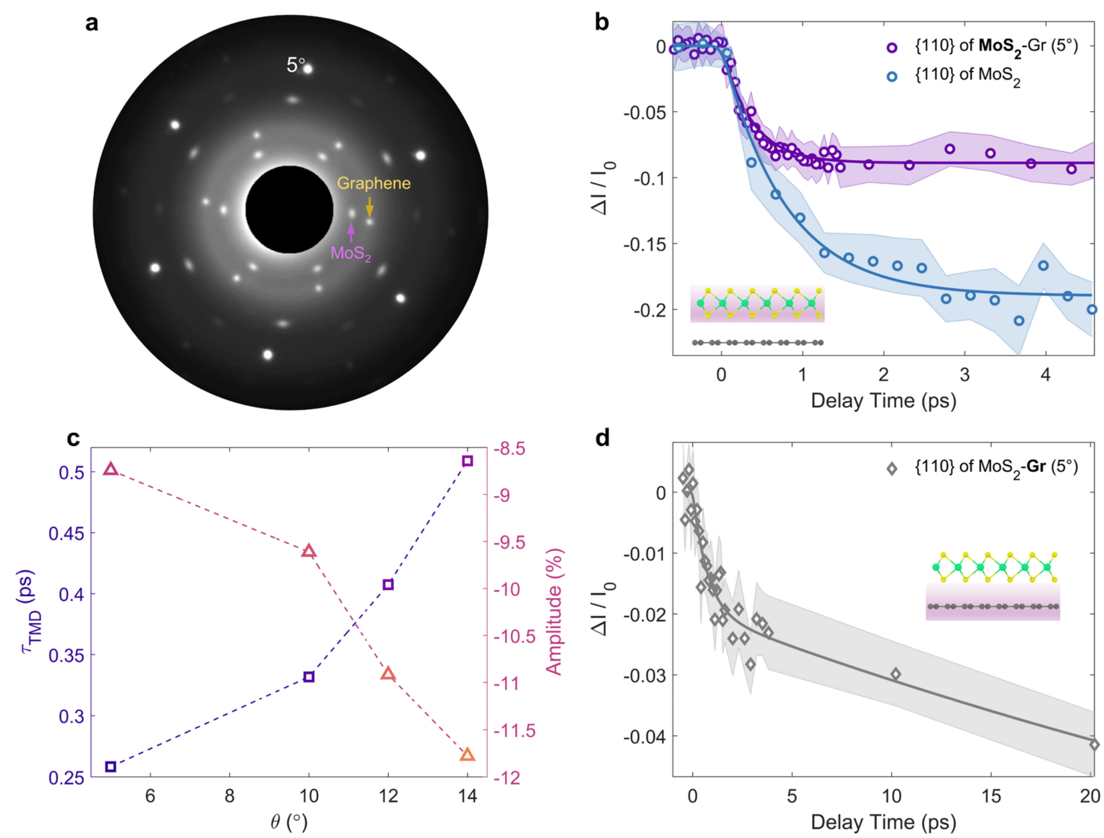

Figure 2. Ultrafast dynamics of MoS_2 and graphene. (a) Typical UED diffraction pattern of MoS_2-graphene heterostructures. (b) Time-resolved diffracted intensity changes of {110} Bragg peaks for MoS_2 in heterostructure and pure monolayer MoS_2. The solid purple line for the heterostructure is a fit from the charge transfer model described below, whereas the solid blue line for the monolayer is a fit to a single exponential decay function. (c) Twist-angle-dependent relaxation time and amplitude of MoS_2 in heterostructures, fitted from a single-exponential decay function. (d) Ultrafast response of graphene in the heterostructure. The solid line is a fit from a biexponential decay function. The shaded area is the error bar showing the standard deviation of the measurements.

scattering spectroscopy.[33−36] Most recently, the energy transfer from TMD to graphene with a characteristic time of ∼3 ps was observed by transient Raman spectroscopy[36] with a temporal resolution >1.4 ps.

In this work, we utilize mega-electronvolt (MeV) ultrafast electron diffraction (UED)[37−42] to directly probe the ultrafast coupled electronic and structural dynamics in prototypical MoS_2-Gr HSs and further reveal the crucial role of twist angle.

MoS_2-Gr HSs samples with different rotation angles were prepared by stacking chemical vapor deposition (CVD)-grown monolayer MoS_2 on mechanically exfoliated graphene layers and then transferring onto grids with amorphous support films (see Supporting Information S1). We pumped MoS_2-Gr HSs with photon energy (3.1 eV) higher than the MoS_2 bandgap. Hot carriers are therefore generated in both MoS_2 and graphene, followed by various intralayer interactions including electron−electron (e-e) scattering, electron−phonon (e-p), and phonon−phonon (p-p) coupling, and interlayer processes such as CT, interlayer Auger, e-p, and p-p coupling in different layers (Figure 1a). MeV electron pulses with ∼100 fs pulse duration are normally incident to the samples, and thus in-plane structural dynamics of the HSs are probed in diffraction (Figure 1b). The top view of a MoS_2-Gr HS with a twist angle of θ is schematically depicted in Figure 1c and the corresponding simulated electron diffraction pattern is shown in Figure 1d. Since the diffracted spots from different component layers are observed and well-separated in the same diffraction pattern, the UED technique enables us to simultaneously trace the ultrafast dynamics of both layers by analyzing the time evolution of selected Bragg peak intensities.

Figure 2a shows a representative UED diffraction pattern of MoS_2-Gr HSs at 5° twist angle, which consists of two sets of 6-fold symmetric diffraction spots corresponding to MoS_2 and graphene, respectively. The twist angles of HSs can be readily determined from the relative rotation of the electron diffraction patterns. No electron beam induced damage was observed during the experiment (Figure S1). We first performed pump−probe measurements on 5° MoS_2-Gr HS and a monolayer MoS_2 sample for comparison. The time-dependent intensities of the MoS_2 diffraction peaks at a fluence of 4 mJ/cm^2 are shown in Figure 2b. Because the six Bragg reflections associated with the same diffraction order show the same behavior, the transients have been obtained by averaging over these six diffraction spots to improve the signal-to-noise ratio (SNR).

The integrated diffraction signals of different order of Bragg peaks exhibit an order-dependent decrease as a function of delay time (Figure S2a). This can be attributed to a laser-induced increase in the random atomic thermal vibrations, capturing the transfer from excited carriers to phonons. These enhanced atomic vibrations, expressed by the atomic mean-square-displacement ($\langle u^2\rangle$, denoted MSD), cause a reduction of Bragg peaks' intensities according to the standard Debye−Waller theory:[37] $\frac{I_{hkl}(\Delta t)}{I_{hkl}^0} = e^{-\Delta\langle u^2\rangle(\Delta t)Q^2}$, where I_{hkl}^0 is the unpumped diffraction signal, scattering vector $Q = 4\pi\sin\,\theta/\lambda$ (θ is the scattering angle and λ is the electron de Broglie wavelength) and $\Delta\langle u^2\rangle$ is the transient change of the MSD upon excitation. According to the previous equation, $\ln\left[\frac{I_{hkl}(\Delta t)}{I_{hkl}^0}\right] = -\Delta\langle u^2\rangle(\Delta t)Q^2$ has a linear dependence on Q^2 with coefficient $-\Delta\langle u^2\rangle(\Delta t)$, as shown in Figure S2b. This observed linear dependence thus shows that the intensity of the Bragg peaks can be used as a proxy for the time-dependent MSDs and thus the time-dependent lattice temperature.

Because of the much higher SNR compared to the high-order spots, we analyzed the dynamics of the more intense {110} family. Within the short timescale window of interest, the transients of bare MoS_2 can be well described by a simple single-exponential decay function[38,39] $\frac{\Delta I}{I_0}(t) = \mathcal{A}(1 - e^{-t/\tau})$. The diffraction intensity signals decreased with a time constant of 0.78 ± 0.11 ps for the {110} family of MoS_2. This timescale is consistent with previous UED measurements on similar TMD crystals[38,39,43] and recent theoretical calculations,[44] where e-p coupling timescales of the order of 1 ps have been reported. Under the same pump/probe conditions, we measured the 5° MoS_2-Gr HS sample, as also shown in Figure 2b. Surprisingly, the structural response of MoS_2 in the HS shows a much faster response than pure monolayer MoS_2. Additionally, there is a noticeable suppression of the magnitude of the effect in the HS compared to monolayer MoS_2 alone (Figure 2b and Figure S3), indicating that energy is being transferred to the graphene layer. Thus, the presence of graphene strongly affects the ultrafast relaxation processes within MoS_2.

To further explore such unusual behaviors, we performed UED measurements on MoS_2-Gr HSs with different twist angles. By fitting the single exponential decay function to the HS data, the timescale and amplitude of ultrafast photoresponse of MoS_2 in heterostructures ($MoS_2^{(HSs)}$) are extracted, as shown in Figure 2c. Remarkably, all time constants of $MoS_2^{(HSs)}$ are much smaller than that from a pure monolayer MoS_2. Moreover, the relaxation timescale of $MoS_2^{(HSs)}$ decreases with decreasing twist angle under the same excitation conditions. The strong interlayer interaction between MoS_2 and graphene is further evidenced by a monotonic reduction of the amplitude of the diffraction change in $MoS_2^{(HSs)}$ as a function of twist, as compared to the monolayer alone (Figure 2c). Separately, the ultrafast photoresponse of graphene within the HS can be obtained by selectively probing the graphene diffraction peaks and fit to a biexponential decay function (Figure 2d). The diffraction intensities decrease with a fast time constant of ∼0.73 ps and a slower one of ∼61 ps, which show a slowing down of the dynamics of graphene in HSs by comparing it with pure monolayer graphene at the same pump conditions (see a more detailed discussion in Supporting Information S4 and Figure S4).

To quantitatively understand how interlayer CT impacts the observed dynamics in MoS_2-Gr HSs, we propose a simple mathematical model to describe the population dynamics of photoexcited carriers and phonons in MoS_2 (see a more detailed discussion in Supporting Information S5), which quantitatively allows one to understand the timescale and amplitude changes discussed above as a function of twist. Because our observations of the photoresponse of $MoS_2^{(HSs)}$ are focused on the short time response, for simplicity, we assume that hot electrons in MoS_2 decay by producing phonons in MoS_2 or transferring to the electronic system, ignoring interlayer e-p and p-p coupling, which typically occur on slower timescales.[30] The following coupled rate equations describe the time-dependent electron and phonon densities in MoS_2:

$$\begin{cases} \dfrac{dn_{p,TMD}}{dt} = r_{ep,TMD}n_{e,TMD} \\ \dfrac{dn_{e,TMD}}{dt} = -r_{ep,TMD}n_{e,TMD} - r_{CT}n_{e,TMD} \end{cases} \tag{1}$$

where $n_{p,\,TMD}$ and $n_{e,\,TMD}$ represent the phonon and carrier densities in MoS_2, $r_{ep,\,TMD}$ is the rate of the e-p process in MoS_2, and r_{CT} is the rate of interlayer CT from MoS_2 to graphene. This approximation assumes that only a single e-p coupling rate plays a role and neglects possible carrier-energy-dependent scattering rates, both of which represent corrections to this model.

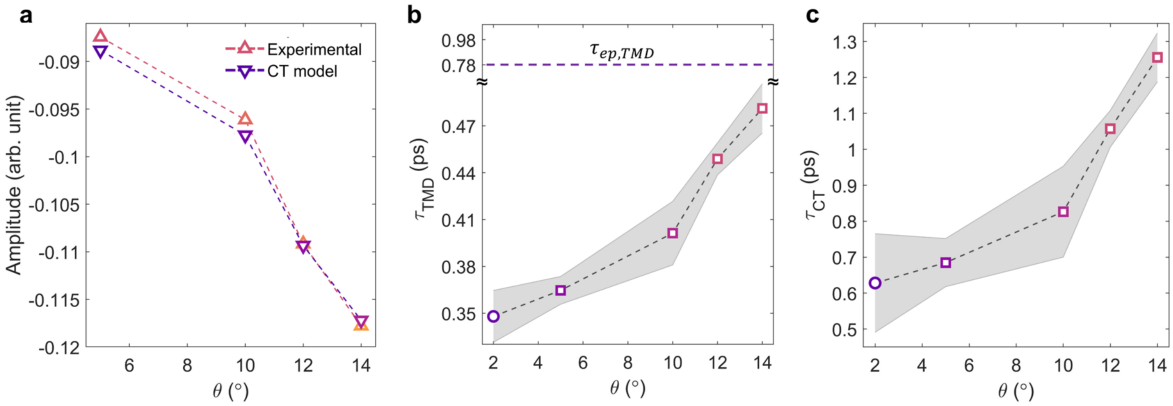

Figure 3. Twist-angle-dependent ultrafast photoresponses. (a) Twist-angle-dependent amplitude change of MoS_2 in HSs. (b) Time constants of MoS_2 in heterostructures as a function of twist angles. The dotted line represents the e-p coupling time of pure monolayer MoS_2, which is much slower than the MoS_2 of HSs. (c) Time constant for CT from MoS_2 to graphene as a function of twist angle. The square data points are pumped with a fluence of 4 mJ/cm^2 and the circle data point are excited with 6 mJ/cm^2. Shaded area: experimental standard deviation.

Nevertheless, we show below that this simple model quantitatively captures the experimental observations.

The solution to eq 1 can be described in two different cases. First, $r_{CT} = 0$ corresponds to the case of bare MoS_2. Its phonon population is then described by

$$n_{p,TMD}(t) = n_{e,TMD}(0)(1 - e^{-r_{ep,TMD}t}) \tag{2}$$

where $n_{e,\,TMD}(0)$ is the initial carrier population created by the pump laser at time zero. Thus, we can fit $\frac{\Delta I}{I} = A_0(1 - e^{-t/\tau_{ep,TMD}})$ to the bare monolayer MoS_2 data to extract the amplitude A_0 (= 0.19) and the relaxation time of intralayer e-p coupling $\tau_{ep,\,TMD}$ (= 0.78 ps) (Figure 2b).

When considering MoS_2-Gr HSs, additional relaxation channels need to be included. When interlayer CT ($r_{CT} \neq 0$) from MoS_2 to graphene occurs, the phonon population of $MoS_2^{(HS)}$ is changed to

$$n_{p,TMD}(t) = \frac{r_{ep,TMD}}{r_{ep,TMD} + r_{CT}} n_{e,TMD}(0)[1 - e^{-(r_{ep,TMD}+r_{CT})t}] \tag{3}$$

Since the e-p coupling of MoS_2 with $\tau_{ep,\,TMD}$ and amplitude A_0 will not significantly change in the HSs, we can modify eq 3 and write it as a function of τ_{TMD}: $\frac{\Delta I}{I} = \frac{\tau_{TMD}}{\tau_{ep,TMD}} A_0(1 - e^{-t/\tau_{TMD}})$, where τ_{TMD} is the overall relaxation time of MoS_2 in HSs, expressed as $\frac{1}{\tau_{TMD}} = \frac{1}{\tau_{ep,TMD}} + \frac{1}{\tau_{CT}}$ where τ_{CT} is the relaxation time of interlayer CT. One can clearly see that the amplitude in the HSs will reduce to $\frac{\tau_{TMD}}{\tau_{ep,TMD}} A_0$ as compared to monolayer (A_0) in agreement with the experimental results.

By fitting the mathematical CT model to the experimental data, we obtain τ_{TMD} = 0.36 ps and amplitude of 0.089 for 5° MoS_2-Gr HS. We thus extract the interlayer CT time finding τ_{CT} = 0.67 ps. As shown in the solid line for the HS in Figure 2b, the CT model fits the experimental data reasonably well. In principle, the generated hot carriers may transfer in both directions between the two layers. However, because the absorption of MoS_2 (~15%) is significantly higher than that of graphene at 3.1 eV[28,45,46] and the graphene Fermi level lies between the MoS_2 valence band and conduction band, more hot carriers are expected to flow into graphene. As indicated by the modified eq 3, the interlayer CT from MoS_2 to graphene provides a new relaxation channel for MoS_2 and leads to a faster relaxation and lower amplitude of the phonon response of the $MoS_2^{(HSs)}$ than that of MoS_2 alone, as experimentally observed.

To further validate the CT model proposed and understand the role of twist angles, we fitted the CT model to the experimental data with different twist angles (Figure S5). As shown in Figure 3a, the extracted magnitude of the change in HSs using the CT model is in good agreement with the experimental amplitude, indicating that the proposed model fits all measured twist angles. The smaller magnitude changes in HSs compared to that in pure MoS_2 shows energy is conserved and indicates the role of interlayer CT. Figure 3b shows the extracted time constants of the second-order Bragg reflections with varying twist angles θ. It shows a similar trend to Figure 2c with the simple single exponential fitting. For all twist angles, the relaxation timescales of MoS_2 in HSs are much smaller than that from a pure monolayer MoS_2. More importantly, it exhibits a strong dependence on twist angles such that the time constants decrease from 0.48 to 0.35 ps with decreasing twist angle (from 14° to 2°). The extracted ultrafast CT of τ_{CT} shows a similar dependence varying from 0.68 to 1.25 ps (Figure 3c). We confirmed that the twist-angle dependence was reproducible in all heterobilayers measured. To rule out the influence of the substrate on the dynamics, we further performed UED measurements on the pure amorphous holey carbon substrate and a 12° MoS_2-Gr HS sample with silicon nitride (SiN) substrate for comparison. By applying the same region of interest to the diffraction pattern of the substrate, no obvious intensity change was observed (Figure S5), indicating no contribution from amorphous carbon (AC) substrate. On the other hand, the ultrafast dynamics of the 12° MoS2-Gr HS sample are consistent with the HS data with AC substrate (Figure S4).

These observations strongly suggest that the interlayer CT can be modulated with a twist. Previous theoretical calculations and experiments have shown that the electronic structure affiliated with the TMD layer is strongly affected by the presence of graphene and found to be twist-angle dependent.[32,47−50] Because the charge transfer occurs mainly through the overlapping between interlayer electronic states, the charge transfer process is believed to be highly dependent on the interlayer stackings and interactions.[23,51,52]

In addition to the interlayer CT, the interlayer Auger process from MoS_2 to graphene could also lead to similar dynamics because the resulting energy from electron−hole pair annihilation in MoS_2 of HSs is transferred to the graphene electronic system. Because the Auger processes involve scattering between two or more charge carriers, the rate of Auger trapping should grow as the pump fluence increases since more charge carriers are produced at higher fluences. Thus, the existence of nonlinear effects can be readily inferred from changes of time constants of $MoS_2^{(HSs)}$ as a function of pump fluence. To better distinguish the contribution of the interlayer CT and Auger process, we further carried out fluence-dependent measurements from 4 to 6 mJ/cm^2 (Figure S7). We first fitted the fluence-dependent data with the CT model by using the same $\tau_{ep,\ TMD}$ and τ_{CT} at 4 mJ/cm^2 and found that the CT model exhibits excellent agreement with the experimental data (Figure S7). This also indicates that e-p coupling and the transfer rate are insensitive to the pump fluence. We then fitted the data with the CT and Auger model and found a slight variation in the matching of the amplitude (see a more detailed discussion in the Supporting Information and Figure S8). No clear changes of time constants of MoS_2 in MoS_2-Gr HSs as a function of pump fluence indicate the nonexistence of nonlinear effects such as Auger processes.[53] These analyses again indicate that ultrafast CT instead of interlayer Auger processes dominate the dynamics in MoS_2-Gr HSs.

In conclusion, the ultrafast carrier and structural dynamics of TMD-graphene heterostructures, and their dependence on interlayer twist angle have been experimentally investigated using MeV UED. The relaxation time of MoS_2 in heterostructures increases monotonically with increasing twist angle and the heterostructures show faster photoresponses than the monolayer MoS_2 alone. The strong interlayer interaction is further supported by changes in the scattering amplitude of MoS_2 and a slowing down of the dynamics of graphene in heterostructures. CT dominates over interlayer Auger processes in all observations. These findings suggest graphene plays a significant role in manipulating the properties of MoS_2. It not only changes the recombination pathway but also provides a knob to tune the photoresponse via twist angle.

AUTHOR INFORMATION

Corresponding Authors

Xiaozhe Shen — *SLAC National Accelerator Laboratory, Menlo Park, California 94025, United States*; Email: xshen@slac.stanford.edu

Guangyu Zhang — *Beijing National Laboratory for Condensed Matter Physics, Key Laboratory for Nanoscale Physics and Devices, Institute of Physics, Chinese Academy of Sciences, Beijing 100190, China*; Email: gyzhang@iphy.ac.cn

Xijie Wang — *SLAC National Accelerator Laboratory, Menlo Park, California 94025, United States*; Email: wangxj@slac.stanford.edu

Aaron M. Lindenberg — *Department of Materials Science and Engineering, Stanford University, Stanford, California 94305, United States; Stanford Institute for Materials and Energy Sciences and Stanford PULSE Institute, SLAC National Accelerator Laboratory, Menlo Park, California 94025, United States*; orcid.org/0000-0003-3233-7161; Email: aaronl@stanford.edu

Authors

Duan Luo — *Department of Materials Science and Engineering, Stanford University, Stanford, California 94305, United States; Stanford Institute for Materials and Energy Sciences, SLAC National Accelerator Laboratory, Menlo Park, California 94025, United States; SLAC National Accelerator Laboratory, Menlo Park, California 94025, United States*; orcid.org/0000-0001-5926-9870

Jian Tang — *Beijing National Laboratory for Condensed Matter Physics, Key Laboratory for Nanoscale Physics and Devices, Institute of Physics, Chinese Academy of Sciences, Beijing 100190, China*

Fuhao Ji — *SLAC National Accelerator Laboratory, Menlo Park, California 94025, United States*

Jie Yang — *SLAC National Accelerator Laboratory, Menlo Park, California 94025, United States*

Stephen Weathersby — *SLAC National Accelerator Laboratory, Menlo Park, California 94025, United States*

Michael E. Kozina — *SLAC National Accelerator Laboratory, Menlo Park, California 94025, United States*

Zhijiang Chen — *SLAC National Accelerator Laboratory, Menlo Park, California 94025, United States*

Jun Xiao — *Department of Materials Science and Engineering, Stanford University, Stanford, California 94305, United States; Stanford Institute for Materials and Energy Sciences, SLAC National Accelerator Laboratory, Menlo Park, California 94025, United States*

Yusen Ye — *Department of Materials Science and Engineering, University of Washington, Seattle, Washington 98195, United States*

Ting Cao — *Department of Materials Science and Engineering, University of Washington, Seattle, Washington 98195, United States*; orcid.org/0000-0003-1300-6084

Author Contributions

D.L., X.Z.S., X.J.W., and A.M.L. designed the research. D.L., X.Z.S., F.H.J., J.Y., and S.W. performed the UED experiments with the laser help of M.E.K. and Z.J.C., J.T., D.L., J.X., and G.Y.Z. prepared the samples. D.L. processed the UED data. D.L., T.C., X.Z.S., X.J.W., and A.M.L. analyzed the data and discussed the results. Y.S.Y, T.C. performed the calculations. D.L. wrote the manuscript with discussion and improvements from all authors.

Notes

The authors declare no competing financial interest.

ACKNOWLEDGMENTS

We thank Dr. Ming-Fu Lin for helpful discussions. This work was primarily funded by the Department of Energy, Office of Science, Basic Energy Sciences, Materials Sciences and Engineering Division, under Contract DE-AC02-76SF00515. The MeV-UED experiments were carried out at SLAC MeV-UED, U.S. Department of Energy Office of Science User Facilities, operated as part of the Linac Coherent Light Source at the SLAC National Accelerator Laboratory, supported by the U.S. Department of Energy, Office of Science, Office of Basic Energy Sciences under Contract DE-AC02-76SF00515. G.Z. acknowledges support from the National Natural Science Foundation of China under Grants 61888102 and 11834017, and the Strategic Priority Research Program of Chinese Academy of Sciences under Grant XDB30000000.

REFERENCES

(1) Geim, A. K.; Grigorieva, I. V. Waals heterostructures. *Nature* **2013**, *499*, 419−425.
(2) Kennes, D. M.; et al. Moiré heterostructures as a condensed-matter quantum simulator. *Nat. Phys.* **2021**, *17*, 155−163.
(3) Liu, Y.; Weiss, N. O.; Duan, X.; Cheng, H.-C.; Huang, Y.; Duan, X. Van der Waals heterostructures and devices. *Nature Reviews Materials* **2016**, *1*, 1−17.
(4) Novoselov, K.; Mishchenko, A.; Carvalho, A.; Castro Neto, A. H. 2D materials and van der Waals heterostructures. *Science* **2016**, *353*, aac9439.
(5) Koppens, F.; et al. Photodetectors based on graphene, other two-dimensional materials and hybrid systems. *Nat. Nanotechnol.* **2014**, *9*, 780.
(6) De Fazio, D.; et al. High responsivity, large-area graphene/MoS_2 flexible photodetectors. *ACS Nano* **2016**, *10*, 8252−8262.
(7) Tao, L.; Chen, Z.; Li, X.; Yan, K.; Xu, J.-B. Hybrid graphene tunneling photoconductor with interface engineering towards fast photoresponse and high responsivity. *npj 2D Materials and Applications* **2017**, *1*, 1−8.
(8) Massicotte, M.; et al. Picosecond photoresponse in van der Waals heterostructures. *Nat. Nanotechnol.* **2016**, *11*, 42−46.
(9) Lorchat, E.; et al. Filtering the photoluminescence spectra of atomically thin semiconductors with graphene. *Nat. Nanotechnol.* **2020**, *15*, 283−288.
(10) Xia, F.; Mueller, T.; Lin, Y.-m.; Valdes-Garcia, A.; Avouris, P. Ultrafast graphene photodetector. *Nat. Nanotechnol.* **2009**, *4*, 839−843.
(11) Bernardi, M.; Palummo, M.; Grossman, J. C. Extraordinary sunlight absorption and one nanometer thick photovoltaics using two-dimensional monolayer materials. *Nano Lett.* **2013**, *13*, 3664−3670.
(12) Britnell, L.; et al. Strong light-matter interactions in heterostructures of atomically thin films. *Science* **2013**, *340*, 1311−1314.
(13) Yuan, L.; et al. Photocarrier generation from interlayer charge-transfer transitions in WS_2-graphene heterostructures. *Science Advances* **2018**, *4*, No. e1700324.
(14) Chen, Y.; Li, Y.; Zhao, Y.; Zhou, H.; Zhu, H. Highly efficient hot electron harvesting from graphene before electron-hole thermalization. *Science Advances* **2019**, *5*, No. eaax9958.
(15) Paul, K. K.; Kim, J.-H.; Lee, Y. H. Hot carrier photovoltaics in van der Waals heterostructures. *Nature Reviews Physics* **2021**, *3*, 178−192.
(16) Yu, L.; et al. Graphene/MoS_2 hybrid technology for large-scale two-dimensional electronics. *Nano Lett.* **2014**, *14*, 3055−3063.
(17) Georgiou, T.; et al. Vertical field-effect transistor based on graphene−WS_2 heterostructures for flexible and transparent electronics. *Nat. Nanotechnol.* **2013**, *8*, 100−103.
(18) Shih, C.-J.; et al. Tuning on−off current ratio and field-effect mobility in a MoS2−graphene heterostructure via Schottky barrier modulation. *ACS Nano* **2014**, *8*, 5790−5798.
(19) Jin, C.; et al. Ultrafast dynamics in van der Waals heterostructures. *Nat. Nanotechnol.* **2018**, *13*, 994−1003.
(20) Dal Conte, S.; Trovatello, C.; Gadermaier, C.; Cerullo, G. Ultrafast photophysics of 2D semiconductors and related heterostructures. *Trends in Chemistry* **2020**, *2*, 28−42.
(21) Sulas-Kern, D. B.; Miller, E. M.; Blackburn, J. L. Photoinduced charge transfer in transition metal dichalcogenide heterojunctions−towards next generation energy technologies. *Energy Environ. Sci.* **2020**, *13*, 2684−2740.
(22) He, R.; Wang, Y.-C.; Wang, X.; Wang, Z.; Liu, G.; Zhou, W.; Wen, L.; Li, Q.; Wang, X.; Chen, X.; et al. Electron transfer and coupling in graphene−tungsten disulfide van der Waals heterostructures. *Nat. Commun.* **2014**, *5*, 1−5.
(23) Wang, Y.; Chen, C. H.; Hu, D.; Ulmschneider, M. B.; Ulmschneider, J. P. The role of collective motion in the ultrafast charge transfer in van der Waals heterostructures. *Nat. Commun.* **2016**, *7*, 1−9.
(24) Chow, C. M.; et al. Unusual exciton−phonon interactions at van der Waals engineered interfaces. *Nano Lett.* **2017**, *17*, 1194−1199.
(25) Jin, C.; et al. Interlayer electron−phonon coupling in WSe_2/hBN heterostructures. *Nat. Phys.* **2017**, *13*, 127−131.
(26) He, J.; He, D.; Wang, Y.; Zhao, H. Probing effect of electric field on photocarrier transfer in graphene-WS_2 van der Waals heterostructures. *Opt. Express* **2017**, *25*, 1949−1957.
(27) Zhang, X.; et al. Electron dynamics in MoS_2-graphite heterostructures. *Nanoscale* **2017**, *9*, 14533−14539.
(28) Wen, S.; Zhou, J.; Zheng, K.; Bednarkiewicz, A.; Liu, X.; Jin, D. Ultrafast probes of electron−hole transitions between two atomic layers. *Nat. Commun.* **2018**, *9*, 1−9.
(29) Tran, M. D.; et al. Decelerated Hot Carrier Cooling in Graphene via Nondissipative Carrier Injection from MoS_2. *ACS Nano* **2020**, *14*, 13905−13912.
(30) Wei, Y.; Lu, M.; Mei, M.; Wang, H.; Han, Z.; Chen, M.; Yao, H.; Song, N.; Ding, X.; Ding, J.; et al. Acoustic phonon recycling for photocarrier generation in graphene-WS_2 heterostructures. *Nat. Commun.* **2020**, *11*, 1−9.
(31) Fu, S.; et al. Long-lived charge separation following pump-wavelength−dependent ultrafast charge transfer in graphene/WS_2 heterostructures. *Science Advances* **2021**, *7*, No. eabd9061.
(32) Ulstrup, S.; et al. Direct observation of minibands in a twisted graphene/WS_2 bilayer. *Science Advances* **2020**, *6*, No. eaay6104.
(33) Du, L.; et al.. Modulating PL and electronic structures of MoS_2/graphene heterostructures via interlayer twisting angle. *Appl. Phys. Lett.* **2017**, *111*, 263106.
(34) Froehlicher, G.; Lorchat, E.; Berciaud, S. Charge versus energy transfer in atomically thin graphene-transition metal dichalcogenide van der Waals heterostructures. *Phys. Rev. X* **2018**, *8*, No. 011007.
(35) Zhang, X.; et al. Twist-angle modulation of exciton absorption in MoS_2/graphene heterojunctions. *Appl. Phys. Lett.* **2019**, *115*, 181901.
(36) Ferrante, C.; Di Battista, G.; López, L. E. P.; Batignani, G.; Lorchat, E.; Virga, A.; Bercuiad, S.; Scopigno, T. Picosecond energy transfer in a transition metal dichalcogenide-graphene heterostructure revealed by transient Raman spectroscopy. *arXiv*, January 14, 2021, 2101.05595. http://arxiv.org/abs/2101.05595.
(37) Sokolowski-Tinten, K.; et al. Electron-lattice energy relaxation in laser-excited thin-film Au-insulator heterostructures studied by ultrafast MeV electron diffraction. *Struct. Dyn.* **2017**, *4*, No. 054501.
(38) Mannebach, E. M.; et al. Dynamic structural response and deformations of monolayer MoS2 visualized by femtosecond electron diffraction. *Nano Lett.* **2015**, *15*, 6889−6895.
(39) Lin, M.-F.; Kochat, V.; Krishnamoorthy, A.; Bassman, L.; Weninger, C.; Zheng, Q.; Zhang, X.; Apte, A.; Tiwary, C. S.; Shen, X.; et al. Ultrafast non-radiative dynamics of atomically thin $MoSe_2$. *Nat. Commun.* **2017**, *8*, 1−8.
(40) Rothenbach, N.; et al. Microscopic nonequilibrium energy transfer dynamics in a photoexcited metal/insulator heterostructure. *Phys. Rev. B: Condens. Matter Mater. Phys.* **2019**, *100*, 174301.
(41) Luo, D.; et al. Ultrafast formation of a transient two-dimensional diamondlike structure in twisted bilayer graphene. *Phys. Rev. B: Condens. Matter Mater. Phys.* **2020**, *102*, 155431.
(42) Gulde, M.; et al. Ultrafast low-energy electron diffraction in transmission resolves polymer/graphene superstructure dynamics. *Science* **2014**, *345*, 200−204.
(43) Waldecker, L.; et al. Momentum-resolved view of electron-phonon coupling in multilayer WSe_2. *Phys. Rev. Lett.* **2017**, *119*, No. 036803.
(44) Caruso, F. Nonequilibrium Lattice Dynamics in Monolayer MoS_2. *J. Phys. Chem. Lett.* **2021**, *12*, 1734−1740.

(45) Ansari, N.; Ghorbani, F. Light absorption optimization in two-dimensional transition metal dichalcogenide van der Waals heterostructures. *J. Opt. Soc. Am. B* **2018**, *35*, 1179−1185.
(46) Li, Y.; et al. Measurement of the optical dielectric function of monolayer transition-metal dichalcogenides: MoS_2, $MoSe_2$, WS_2, and WSe_2. *Phys. Rev. B: Condens. Matter Mater. Phys.* **2014**, *90*, 205422.
(47) Jin, W.; et al. Tuning the electronic structure of monolayer graphene/MoS_2 van der Waals heterostructures via interlayer twist. *Phys. Rev. B: Condens. Matter Mater. Phys.* **2015**, *92*, 201409.
(48) Wang, Z.; Chen, Q.; Wang, J. Electronic structure of twisted bilayers of graphene/MoS_2 and MoS_2/MoS_2. *J. Phys. Chem. C* **2015**, *119*, 4752−4758.
(49) Ulstrup, S.; et al. Ultrafast band structure control of a two-dimensional heterostructure. *ACS Nano* **2016**, *10*, 6315−6322.
(50) Pierucci, D.; et al. Band alignment and minigaps in monolayer MoS_2-graphene van der Waals heterostructures. *Nano Lett.* **2016**, *16*, 4054−4061.
(51) Zhang, J.; et al. Interlayer-state-coupling dependent ultrafast charge transfer in MoS_2/WS_2 bilayers. *Advanced Science* **2017**, *4*, 1700086.
(52) Geng, W.; Wang, V.; Lin, J.; Ohno, T.; Nara, J. Angle Dependence of Interlayer Coupling in Twisted Transition Metal Dichalcogenide Heterobilayers. *J. Phys. Chem. C* **2021**, *125*, 1048−1053.
(53) Cunningham, P. D.; McCreary, K. M.; Jonker, B. T. Auger recombination in chemical vapor deposition-grown monolayer WS_2. *J. Phys. Chem. Lett.* **2016**, *7*, 5242−5246.